nature neuroscience

Patterned expression of Purkinje cell glutamate transporters controls synaptic plasticity

Jacques I Wadiche & Craig E Jahr

Glutamate transporters are responsible for clearing synaptically released glutamate from the extracellular space. If expressed at high enough densities, transporters can prevent activation of extrasynaptic receptors by rapidly lowering glutamate concentrations to insignificant levels. We find that synaptic activation of metabotropic glutamate receptors expressed by Purkinje cells is prevented in regions of rat cerebellum where the density of the glutamate transporter EAAT4 is high. The consequences of metabotropic receptor stimulation, including activation of a depolarizing conductance, cannabinoid-mediated presynaptic inhibition and long-term depression, are also limited in Purkinje cells expressing high levels of EAAT4. We conclude that neuronal uptake sites must be overwhelmed by glutamate to activate perisynaptic metabotropic glutamate receptors. Regional differences in glutamate transporter expression affect the degree of metabotropic glutamate receptor activation and therefore regulate synaptic plasticity.

At excitatory synapses, termination of the actions of synaptically released glutamate depends both on its diffusion out of the cleft and on its uptake by glutamate transporters expressed by neurons and astrocytes. Astrocytic transporters provide the main sink for glutamate uptake in most regions of the CNS, whereas the neuronal transporters are responsible for only a small fraction of the released transmitter[1–3]. Indeed, genetic disruption of astrocytic transport can cause striking pathologies[4] that contrast with the subtle effects seen when neuronal transporters are blocked or knocked out[5–7]. Despite numerous studies of both neuronal and astrocytic uptake[2], the physiological function of glutamate transporters has been inferred only after pharmacological or genetic disruption. Studies of regulation or trafficking of glutamate transporters have not found physiological conditions in which synaptic glutamate uptake is modulated[8,9]. In spite of this, controlling the rate of uptake by altering the kinetics or densities of transporters located near synapses remains an attractive mechanism to adjust synaptic strength and the activation of extrasynaptic receptors.

Cerebellar Purkinje cells express two isoforms of neuronal transporters, excitatory amino acid transporters 3 and 4 (EAAT3 and EAAT4). The Purkinje cell–specific transporter EAAT4 is located at high densities in the membranes of postsynaptic spines surrounding the cleft and is responsible for the vast majority of Purkinje cell uptake[2]. Despite the dense expression of transporters in nearby Bergmann glial membranes, EAAT4 transporters control the activation of perisynaptic metabotropic glutamate receptors (mGluRs) in Purkinje cells[5]. In this study, we determine the occupancy of Purkinje cell transporters at two cerebellar synapses. We find that the efficacy of glutamate clearance by Purkinje cell transporters is not the same in different regions of cerebellum. These differences are correlated with the differential expression of EAAT4 in these regions. In regions of high EAAT4 expression, more effective clearance of glutamate largely prevents metabotropic receptor activation and thus limits both short- and long-term synaptic plasticity associated with extrasynaptic receptor activation.

RESULTS

Synaptic Purkinje cell transporter occupancy depends on location

Climbing fiber stimulation elicits a synaptic current in Purkinje cells mediated by AMPA receptors (AMPARs)[10–12] and, to a much smaller extent, kainate receptors[7] and EAATs[13]. The portion mediated by EAATs, the synaptic transport current (STC), is enhanced by solutions containing permeant anions such as nitrate[3,13–15] and can be used to measure the relative number of transporters activated in different conditions[16]. We used nitrate-enhanced climbing fiber STCs to monitor the occupancy of Purkinje cell transporters after synaptic stimulation.

Increasing extracellular Ca^{2+} from 2 to 5 mM increases release of glutamate at climbing fiber–Purkinje cell synapses[12]. However, the same manipulation produced a variable enhancement of the climbing fiber-Purkinje cell STC in only half of the recordings (**Fig. 1a**). This suggests that in the Purkinje cells showing no enhancement, transporters close to release sites were nearly saturated by glutamate in 2 mM Ca^{2+}. In these Purkinje cells, the increased release of glutamate in 5 mM Ca^{2+} does not result in binding of greater numbers of Purkinje cell EAATs but rather is absorbed by the excess transport capacity of the surrounding Bergmann glial cells[17]. The differences may be explained by the variation in the density of EAAT4 expression, the Purkinje cell–specific transporter. For unknown reasons, EAAT4 expression shows

Vollum Institute, Oregon Health and Science University, L474, 3181 SW Sam Jackson Park Road, Portland, Oregon 97239-3098, USA. Correspondence should be addressed to C.E.J. (jahr@ohsu.edu).

Received 27 May; accepted 16 August; published online 4 September 2005; doi:10.1038/nn1539

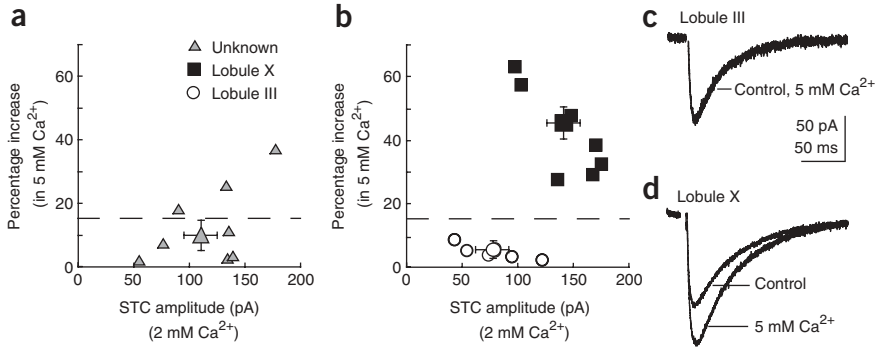

Figure 1 Purkinje cell location predicts transporter number and occupancy following climbing fiber activation. (**a**) Percentage increase in STC amplitude by increasing extracellular Ca^{2+} (from 2 to 5 mM) versus STC amplitude in 2 mM Ca^{2+}. Each point represents values from a Purkinje cell in an unknown location (triangles) in the cerebellar vermis. Dotted line denotes a 15% increase in STC amplitude. The mean ± s.e.m. is represented by the large symbol and error bars. (**b**) Same as in **a** but from Purkinje cells in lobule III (circles) or lobule X (squares) in the cerebellar vermis. (**c**,**d**) Climbing fiber–Purkinje cell STCs (25 μM NBQX) in control (2 mM Ca^{2+}) and in 5 mM Ca^{2+} from Purkinje cells in lobule III (**c**) and lobule X (**d**).

parasagittal patterns similar to those of the unrelated protein zebrin II (refs. 18–20). This contrasts with the homogeneous expression of glutamate transporters in Bergmann glial membranes[19,21]. In keeping with this, climbing fiber–Purkinje cell STCs recorded in lobule X, a cerebellar region where the majority of Purkinje cells express zebrin II (ref. 22), were significantly larger than STCs from lobule III (**Fig. 1** and **Table 1**), a region largely devoid of zebrin II^+ Purkinje cells[22]. Similar results were found when the experiments were done at elevated temperatures (32–35 °C) using a K^+-based intracellular solution. In these conditions, the STC amplitudes in lobule X were twofold larger than those in lobule III (249.1 ± 14.9 and 156.8 ± 26.4 pA; respectively, $n = 6$ and 5; $P = 0.018$).

The STCs recorded in lobules III and X were differentially affected by changes in release probability. In lobule III, a region with a lower density of EAAT4, the STC was less affected by increasing extracellular Ca^{2+} than the STCs recorded from Purkinje cells in lobule X (6.5 ± 1.7% and 45 ± 7.6%; respectively, $n = 5$ and 7; $P = 0.0006$; **Fig. 1b–d**). Across all cells, the STC amplitude increase after switching into 5 mM Ca^{2+} was not dependent on the initial STC amplitude in 2 mM Ca^{2+} (**Fig. 1a**,**b**). This indicates that the number of active Purkinje cell transporters (or number of release sites) does not predict the occupancy of transporters after climbing fiber stimulation.

We suggest that these differences result from different expression levels of EAAT4 transporters located near synapses. However, they could also represent differences in the ability of climbing fibers in these regions to regulate release probability. To test this, we recorded climbing fiber–Purkinje cell AMPAR-mediated excitatory postsynaptic currents (EPSCs) in lobules III and X in the presence of the low-affinity AMPAR antagonist γ-D-glutamylglycine (γ-DGG; 2 mM) to prevent AMPAR saturation and allow for a more linear relationship between the synaptic glutamate concentration and the EPSC amplitude[12,23]. In this condition, climbing fiber–Purkinje cell EPSC amplitude and paired-pulse ratio were not different in the two regions (**Table 1**). In addition, the amount of inhibition by γ-DGG was similar in these two cerebellar regions (**Table 1**). Furthermore, increases in climbing fiber–Purkinje cell EPSCs resulting from elevation of extracellular Ca^{2+} were not different across lobules (**Fig. 2a**,**b**). EPSCs increased to 45 ± 16% and 55 ± 8.2% in lobule III and lobule X, respectively (**Fig. 2c**, $n = 6$ and 8; $P = 0.53$). These results indicate that neither release probability nor regulation of release probability can account for the different behavior of climbing fiber–Purkinje cell STCs in lobules III or X.

Are these regional differences restricted to climbing fiber synapses or can they also be detected after release from parallel fiber synapses onto Purkinje cells? Parallel fiber–Purkinje cell AMPAR-mediated EPSCs in lobule III or lobule X were evoked with stimulus intensities adjusted to keep the EPSCs below 500 pA. Similar to climbing fiber stimulation, parallel fiber-Purkinje cell EPSCs from the two cerebellar regions were not distinguishable (**Fig. 3a**,**b**,**d**). Parallel fiber EPSCs in the two regions had similar paired-pulse ratios (1.7 ± 0.09 and 1.8 ± 0.07 in lobules III and X, respectively; $n = 7$ each; $P = 0.38$). Without changing the stimulus intensity, NBQX (10 μM) was added to block AMPAR-mediated EPSCs. In lobule X, the parallel fiber–evoked currents after AMPAR blockade had characteristics similar to climbing fiber–Purkinje cell STCs: slow activation and decay (**Fig. 3b**,**c**). These currents did not reverse at positive potentials, as expected of transporter currents in these conditions, and were inhibited by the transporter antagonist TBOA (**Fig. 3c**, 100 μM, 91.6 ± 7.4% block, $n = 4$)[24]. The result was distinctly different in lobule III, where the response in NBQX consisted mainly of a small, fast current (**Fig. 3a**,**c**). Increasing the stimulus intensity or the number of stimuli resulted in a slow, long-lasting current of similar time course to STCs in lobule X (data not shown). This suggests that neuronal transporters are present in these Purkinje cells but that release from more parallel fiber synapses and therefore increased glutamate pooling is required to activate them in significant numbers. We quantified the results in both regions by measuring the peak currents following NBQX block. The parallel fiber–evoked peak currents in NBQX (measured at 10 ms after the stimulus) were 28.4 ± 5.5 pA in lobule X and 9.0 ± 1.2 pA in lobule III

Table 1 Comparison of climbing fiber–Purkinje cell STC and climbing fiber–Purkinje cell EPSC

	STC amplitude (pA)	STC rise (ms)	STC weighted decay τ (ms)	EPSC amplitude (nA)	EPSC PPR	γ-DGG block
Lobule III	77.2 ± 14.1 (7)*	3.0 ± 0.5 (6)	60.1 ± 5.7 (5)	4.2 ± 0.7 (4)	0.51 ± 0.05 (4)	0.48 ± 0.06 (4)
Lobule X	141.7 ± 12.1 (7)*	2.6 ± 0.6 (7)	59.9 ± 5.3 (5)	4.7 ± 1.3 (5)	0.57 ± 0.04 (5)	0.53 ± 0.02 (5)

Climbing fiber–evoked STCs were recorded from Purkinje cells (–60 to –70 mV). STC rise is the 20 to 80% rise time. STC weighted decay τ is the double exponential fit of the decay phase ((percentage $amplitude_{fast} \times \tau_{fast}$) + (percentage $amplitude_{slow} \times \tau_{slow}$)). The STC amplitude in lobules III and X were significantly different (*, $P < 0.005$). Climbing fiber EPSCs were recorded from Purkinje cells at –15 mV. EPSC paired pulse ratios (PPRs) were measured with an interstimulus interval of 100 ms. The γ-DGG (2 mM) block was measured as the fractional current blocked. Numbers in parentheses represent number of cells tested.

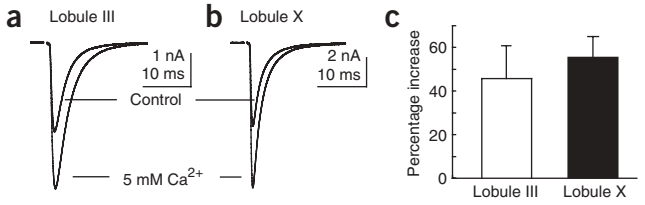

Figure 2 Release probability is not dependent on Purkinje cell location. (**a**,**b**) Climbing fiber–Purkinje cell EPSCs (in γ-DGG; 2 mM) in control (upper traces, 2 mM Ca^{2+}) and in 5 mM Ca^{2+} (lower traces) from lobule III (**a**) and lobule X (**b**). (**c**) Percentage increase in EPSC amplitude after elevation of extracellular Ca^{2+} (from 2 to 5 mM) in lobule III and lobule X.

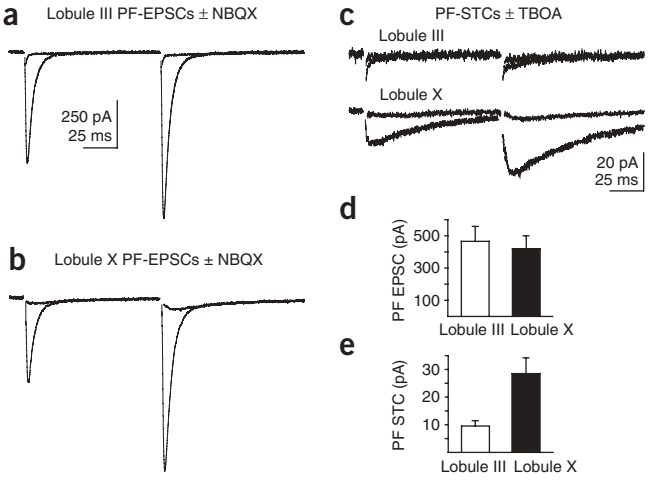

Figure 3 Purkinje cell location predicts transporter number following parallel fiber (PF) activation. (**a**,**b**) Parallel fiber–Purkinje cell EPSCs and STCs before (lower traces) and after the addition of NBQX (25 μM, upper traces) in lobule III (**a**) and lobule X (**b**). (**c**) Parallel fiber–Purkinje cell STCs from lobule III and lobule X at higher gain before (lower traces) and after (upper traces) the addition of TBOA (100 μM). (**d**,**e**) EPSC and STC peak amplitudes following parallel fiber activation from Purkinje cells located in lobule III (**d**) and lobule X (**e**).

($n = 7$ each, $P = 0.005$; **Fig. 3e**). In keeping with our climbing fiber STC results, we conclude that the density of Purkinje cell transporters at parallel fiber synapses is higher in lobule X than in lobule III.

Functional role for neuronal uptake

Purkinje cell transporters regulate Purkinje cell mGluR activation[5]. This interaction seems to result from the overlapping postsynaptic distributions of EAAT4 and mGluR1 (refs. 19,25). Trains of parallel fiber stimuli elicit a slow synaptic depolarizing potential in Purkinje cells resulting from the activation of perisynaptic mGluRs[26]. Recent evidence indicates that the membrane conductance change responsible for this slow EPSP depends on the activation of the cation channel TRPC1 (ref. 27). This mGluR-mediated conductance varies tremendously from Purkinje cell to Purkinje cell in both size and waveform[5,28]. We tested whether this variability resulted from differences in Purkinje cell transporter density. mGluR-mediated currents were evoked by trains of parallel fiber stimuli (ten stimuli, 100 Hz) in the presence of NBQX (10–25 μM). In lobule III Purkinje cells, where EAAT4 expression is low, robust mGluR currents were elicited (**Fig. 4a**). In contrast, the mGluR currents recorded from lobule X Purkinje cells were much smaller in amplitude (**Fig. 4b**). Currents in both lobules were blocked by subsequent bath application of CPCCOEt, a selective mGluR1 antagonist (100 μM; 94.5 ± 1.3%; $n = 10$; **Fig. 4a**,**b**). The amplitudes of the mGluR-mediated currents were compared with the AMPAR-mediated EPSC evoked in the same cells by a single stimulus of the same intensity as those administered in the train, before application of NBQX (**Fig. 4c**). mGluR-mediated currents from lobule III Purkinje cells were larger than those from lobule X Purkinje cells for an EPSC of a given amplitude (mGluR-EPSC/AMPAR-EPSC ratios were 0.21 ± 0.03 and 0.06 ± 0.009 in lobule III and lobule X, respectively; $n = 22$ and 23; $P < 0.0001$).

To control for possible differences in mGluR expression across cerebellar regions, we performed two sets of experiments. First, we focally applied the mGluR agonist DHPG (100 μM). AMPA (1 mM) was added to the DHPG application pipette so that AMPAR-mediated currents could be used to position the puffer pipette. Currents elicited by brief application of both agonists were biphasic (**Fig. 5a**). We confirmed that NBQX (25 μM) blocked the first, fast response (93.2 ± 2.7%, $n = 4$), whereas the mGluR1-selective antagonist CPCCOEt (100 μM) blocked the slow response (95.1 ± 3.1%, $n = 5$), as has been previously shown[27]. The amplitude of the DHPG current was similar in lobules III and lobule X, respectively (610 ± 67 and 547 ± 39 pA, $n = 6$ and 8; $P = 0.41$; **Fig. 5b**). In a second set of control experiments, we compared synaptically evoked mGluR EPSCs in the two lobules in the presence of TBOA, a nonselective glutamate uptake blocker. First, parallel fiber AMPAR EPSCs of similar amplitudes were evoked by adjusting the stimulus intensity (506 ± 48.5 and 533 ± 92.2 pA in lobules III and X, respectively; $n = 9$; $P = 0.8$; **Fig. 5d**). Without changing the stimulus intensity, NBQX (10–20 μM) was added to block AMPAR-mediated EPSCs while trains of stimuli were given to elicit parallel fiber mGluR EPSCs as in **Figure 4** (**Fig. 5c**). Next, we added TBOA to block uptake (see Methods). With uptake blocked, the parallel fiber mGluR EPSCs from Purkinje cells located in the two lobules were not different (262.2 ± 52.4 and 236.8 ± 66.8 pA in lobules III and X, respectively; $n = 9$ each; $P = 0.77$; **Fig. 5e**).

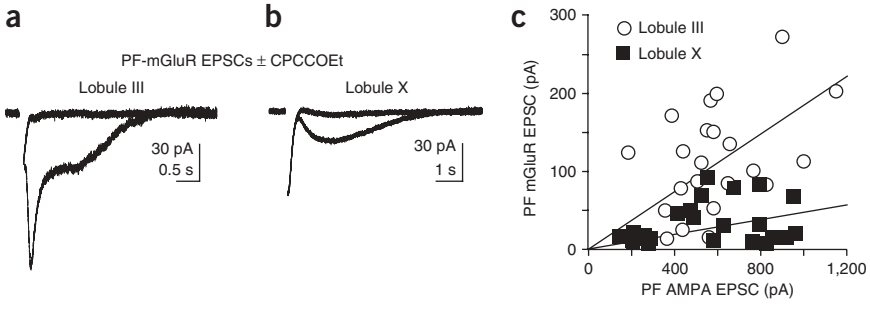

Figure 4 Parallel fiber (PF)–Purkinje cell mGluR currents depend on Purkinje cell location. (**a**,**b**) Parallel fiber–Purkinje cell mGluR EPSCs following a train of stimuli (100 Hz, ten stimuli) after AMPAR EPSCs were blocked (10 μM NBQX) in lobule III (**a**) and lobule X (**b**). mGluR EPSCs were blocked by CPCCOEt (100 μM, upper traces). (**c**) Correlation of parallel fiber–Purkinje cell AMPAR EPSC amplitude following a single stimulus and parallel fiber–Purkinje cell mGluR EPSC (10 μM NBQX; 100 Hz, ten stimuli) in lobule III (circles) and lobule X (squares). The lines represent the best linear fit.

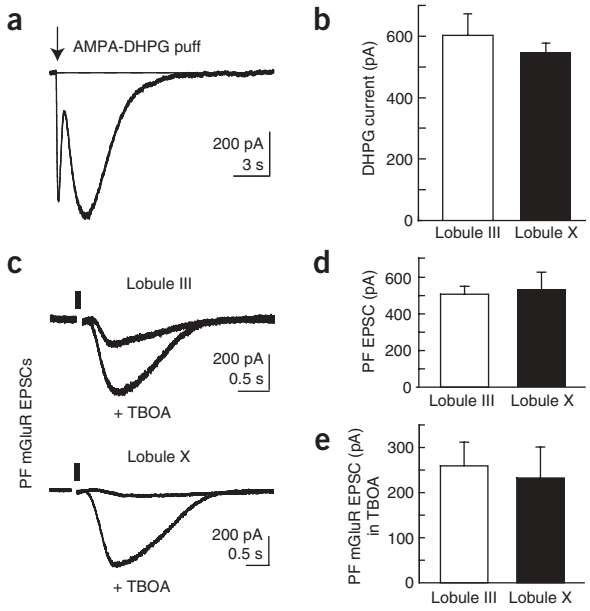

Figure 5 Purkinje cell mGluR sensitivity does not depend on cell location. (**a**) Currents elicited by co-application (arrow) of AMPA (1 mM) and DHPG (100 μM). (**b**) Summary of peak DHPG-sensitive current after puff application in Purkinje cells from lobule III and lobule X. (**c**) Parallel fiber (PF)–Purkinje cell mGluR EPSCs recorded in Purkinje cells in lobules III and X (100 Hz, ten stimuli) in the presence of NBQX (20 μM) ± TBOA (100 μM). (**d**) Amplitudes of single stimulus–evoked parallel fiber-Purkinje cell AMPAR EPSCs before the addition of NBQX in the two lobules. (**e**) Amplitudes of parallel fiber–Purkinje cell mGluR EPSCs in the presence of NBQX and TBOA.

Together, these experiments indicate that synaptically evoked and dendritic mGluRs, and their downstream effectors, are not differentially expressed across cerebellar regions.

Regional differences in synaptic plasticity

Trains of parallel fiber action potentials cause an endocannabinoid-mediated modulation of spontaneous IPSCs that requires activation of Purkinje cell mGluRs[29]. As our results indicate that activation of Purkinje cell mGluRs depends on the expression of Purkinje cell transporters, we tested whether the strength of endocannabinoid-mediated inhibition differs in the two cerebellar regions. We monitored the effect of parallel fiber stimulation (ten stimuli, 100 Hz) on the frequency of spontaneous inhibitory postsynaptic currents (sIPSCs) recorded in Purkinje cells in the presence of NBQX (10 μM; **Fig. 6a–d**). In Purkinje cells from lobule III, the stimulation typically elicited an mGluR EPSC, in keeping with our previous observations (**Figs. 4** and **5**). The frequency of sIPCSs increased immediately after stimulation; this was followed by a depression of sIPSC frequency that lasted for ~10 s, as previously reported[29] (25.2 ± 5.3%; $n = 8$; **Fig. 6a,c**). The mGluR1 antagonist CPCCOEt (100 μM; 2.6 ± 6.4%; $n = 4$; $P < 0.05$; ANOVA) or the cannabinoid receptor antagonist AM-251 (1–5 μM; 5.7 ± 3.9%; $n = 6$; $P < 0.05$; ANOVA) blocked this depression. In lobule X, however, parallel fiber stimulation produced a small or non-existent mGluR-mediated current and significantly less depression of sIPSCs frequency than in lobule III (3.5 ± 3.5%; $n = 5$; $P = 0.013$; **Fig. 6b,d**). We confirmed that direct Purkinje cell depolarization could induce endocannabinoid-mediated depression of sIPSCs (DSI)[30] to similar levels in both lobules (34.6 ± 7.2% and 29.6 ± 6.0% in lobule III and X respectively; $n = 5$ each; $P = 0.61$).

We also tested whether long-term synaptic depression (LTD) of parallel fiber synapses on Purkinje cells[31–33] was affected by the regional differences in neuronal transporter density. LTD requires the activation of mGluRs expressed by Purkinje cells and results in a reduction of AMPAR-mediated EPSCs at parallel fiber synapses[33–35]. LTD of parallel fiber–mediated AMPAR EPSCs was induced by pairing parallel fiber stimulation and Purkinje cell depolarization (see Methods). In lobule X, this pairing protocol did not induce LTD (6.5 ± 10.9% depression versus baseline, response measured at $t = 15$–20 min, $n = 8$; **Fig. 6e**). This contrasts with the result in lobule III, where the pairing protocol resulted in robust LTD (39.1 ± 7.6%, depression, $n = 6$; $P = 0.041$; **Fig. 6e**). Notably, combining all cells from both cerebellar regions resulted in a more modest LTD (20.5 ± 8.1%; $n = 14$), similar to published values for parallel fiber LTD[5,31,35].

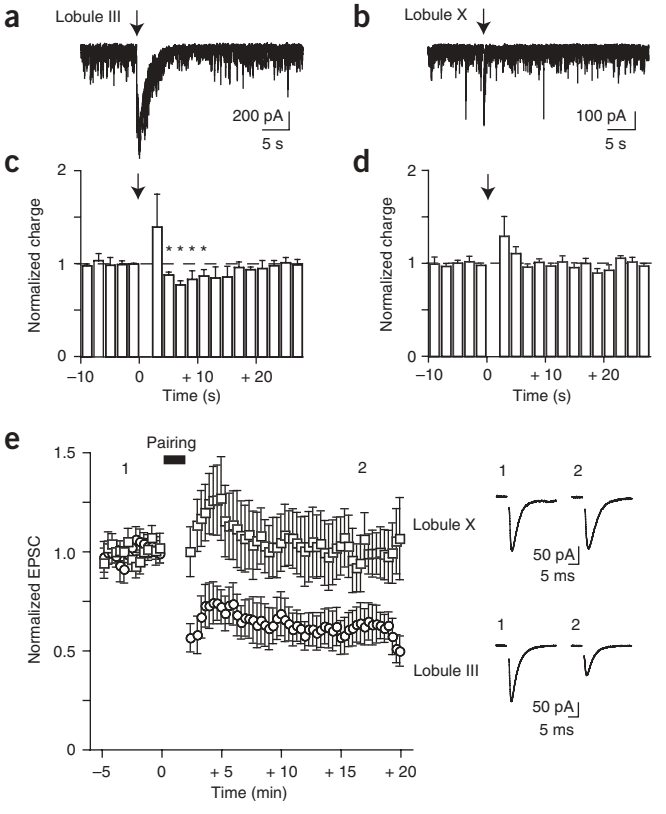

Figure 6 Regional differences in mGluR-mediated synaptic plasticity. (**a**,**b**) sIPSCs in Purkinje cells (10 μM NBQX) after a train of parallel fiber stimuli (100 Hz, ten stimuli, arrow) in lobule III and lobule X. Note that a parallel fiber–evoked mGluR-mediated EPSC was present only in the recording from the lobule III Purkinje cell. (**c**,**d**) Cumulative time integral of sIPSCs (2-s bins) for all experiments before and after parallel fiber train stimulation (arrow) in recordings from Purkinje cells located in lobule III and lobule X. Note the depression in sIPSC charge that persists for several seconds after parallel fiber stimulation is present only in Purkinje cells from lobule III. (**e**) Comparison of LTD in two groups of Purkinje cells elicited by the same protocol (pairing protocol given at $t = 0$). Normalized (first 5 min) mean peak amplitude of parallel fiber–evoked AMPAR-mediated EPSCs are plotted against time for Purkinje cells located in lobule X (squares) and lobule III (circles). Example traces before (point 1) and after (point 2) the pairing protocol from a Purkinje cell in lobule X (top) and a Purkinje cell in lobule III (bottom), respectively. Experiments were done at 32–34 °C.

Together with the cannabinoid-mediated inhibition of sIPSC frequency, these results indicate that Purkinje cell transporter density not only affects mGluR activation but also acts as a physiological gatekeeper, regulating feedback to presynaptic structures and Purkinje cell AMPAR expression in a model of plasticity.

DISCUSSION

We show that synaptic stimulation of climbing fibers or parallel fibers can overwhelm neuronal transporters in a subset of cerebellar Purkinje cells. This insufficiency of transport results in activation of mGluRs and presynaptic inhibitory feedback. A separate population of Purkinje cells express higher levels of transporters that are not saturated by release; this prevents mGluR activation, presynaptic feedback and long-term depression. These two populations of Purkinje cells reside in discrete locations, resulting in a banding pattern in the cerebellum[18–20,22]. Our results describe functional consequences of this patterned gene expression.

Functional consequences of glutamate transporter density

On the basis of the amplitudes of Purkinje cell STCs, we suggest that Purkinje cells in lobule X express more than twice the density of transporters than Purkinje cells in lobule III. The difference in transporter density may be an underestimate because the large transporter currents in lobule X may be limited by release rather than by transporter density. The intrinsic difference in the number of glutamate transporters has physiological consequences because of the overlapping distribution of EAAT4 and mGluRs in the perisynaptic regions of Purkinje cell spines. In lobule III, synaptically released glutamate can overwhelm Purkinje cell transporters, leading to the activation of mGluRs. Purkinje cells that express fewer transporters are therefore more susceptible to forms of synaptic plasticity that require activation of mGluRs, whereas plasticity is limited in Purkinje cells that express abundant transporters.

Synaptic plasticity

We have described differences in mGluR-mediated short- and long-term synaptic plasticity resulting from the differential distribution of EAAT4. Other aspects of plasticity[33,36] and synapse elimination[37,38] that depend on mGluRs may also be influenced by the expression pattern of neuronal transporters. Physiological activation of perisynaptic mGluRs leads to Ca^{2+} signaling that is restricted to discrete locations[39,40]. Even during intense periods of synaptic activity at climbing fiber and parallel fiber inputs, Purkinje cells expressing high densities of transporters will experience smaller mGluR-mediated Ca^{2+} signals and therefore less long-term depression of parallel fiber synaptic transmission, a process thought to mediate some forms of cerebellar learning[33,36]. In addition, a discrete phase of synapse elimination between climbing fibers and Purkinje cells has an mGluR-dependent component[37]. These authors suggested that synaptic activity leading to mGluR activation generates a signal that results in elimination of multiple climbing fibers. Whether Purkinje cells with a high density of glutamate transporters are more likely to remain innervated by multiple climbing fibers[41] remains to be determined.

Pattern formation and differentiation in cerebellum

The stereotypical cytoarchitecture of the cerebellum has led the view that all cerebellar Purkinje cells behave similarly despite the existence of distinct patterns of gene expression[18–20,42–44]. Our results, and the banded distribution of EAAT4 and zebrin II (refs. 18–20), suggest that discrete areas in the cerebellum may have physiologically distinct properties[19]. In support of this hypothesis, Purkinje cells with a dearth of EAAT4 and zebrin II expression are more susceptible to excitotoxicity after global brain ischemia[20]. Furthermore, Purkinje cells with low EAAT4 and zebrin II expression are protected from ischemic excitotoxicity by transection of their climbing fiber input[20]. This suggests that synaptic release of glutamate after brain ischemia more easily kills Purkinje cells with lower densities of EAAT4 transporters. Thus, it seems that the density of EAAT4 expression may be important not only in cerebellar development and plasticity but also in pathological states.

The value of neuronal uptake

In the CNS, it is generally agreed that astrocytic transporters are responsible for the majority of glutamate uptake[1–3]. Recently, however, several studies have reported that neuronal transporters can have significant effects. Neuronal transporters are generally expressed at far lower densities than their glial counterparts[2]. Studies in cerebellum[5,45] and hippocampus[6,46] suggest that the low-capacity neuronal uptake systems serve to regulate glutamate concentration near release sites. In Purkinje cells, EAAT4 is closely associated with intracellular proteins (glutamate transporter–associated proteins or GTRAPs) that specifically interact with the intracellular domain of EAAT4 and modulate its transport activity[8]. GTRAPs are thought to interact with the actin cytoskeleton and stabilize or anchor EAAT4 at the cell membrane. The effects seen in this study may be attributed to the expression levels of GTRAP, a notion yet to be investigated. Determining the mechanisms that control expression and trafficking of EAAT4 in Purkinje cells is central to understanding cerebellar development and function.

METHODS

Tissue preparation. Parasagittal cerebellar slices were prepared from P12–21 rats[10]. Animals were anesthetized with halothane and then decapitated in accordance with the Oregon Health and Science University Institutional Animal Care and Use Committee. The cerebellar vermis was dissected out and glued to the stage of a vibroslicer (Leica) in ice-cold solution containing (in mM) 119 NaCl, 2.5 KCl, 2 $CaCl_2$, 1 $MgCl_2$, 1 NaH_2PO_4, 26.2 $NaHCO_2$ and 11 glucose, bubbled with 95% O_2/5% CO_2. Slices 250- to 300-μm-thick were cut and incubated at 35 °C for 30 min before use in electrophysiological recordings. During recordings, the slices were superfused with the solution described above.

Electrophysiology. Whole-cell recordings with pipettes of 1 to 1.5 MΩ resistance were made using infrared differential interference contrast optics and a 40× water immersion objective on an upright microscope (Zeiss Axioskop). The series resistance, as measured by the instantaneous current response to a 1–5 mV step with only the pipette capacitance cancelled, was always less than 7 MΩ (usually less than 5 MΩ) and was compensated >80%. Pipette solutions contained (in mM) 130 $CsNO_3$, 10 EGTA, 10 HEPES, 0.5 $MgCl_2$ or 130 KNO_3, 10 NaCl, 10 HEPES, 1 EGTA, 10 Tris-phosphocreatine, 2 ATP (Mg) and 0.4 GTP (Na) for STCs. mGluR EPSCs were recorded with either 130 $CsNO_3$, 10 EGTA, 10 HEPES and 0.5 $MgCl_2$, or 130 CsCl, 10 TEACl, 10 HEPES, 1 EGTA, 10 Tris-phosphocreatine, 2 ATP (Mg) and 0.4 GTP (Na). IPSCs were recorded with 130 CsCl, 10 TEACl, 10 HEPES, 1 EGTA, 10 Tris-phosphocreatine, 2 ATP (Mg) and 0.4 GTP (Na). Climbing fiber–Purkinje cell EPSCs were recorded at –10 mV, and parallel fiber–Purkinje cell EPSCs (AMPAR or mGluR) were recorded at –70 mV. Synaptic transporter currents were recorded at –70 mV in the presence of 10–100 μM NBQX and 5 μM SR95531. Climbing fibers were stimulated (5–50 V, 50–100 μs) with a theta glass pipette filled with bath solution, placed in the granule cell layer. To eliminate significant parallel fiber activation, the stimulating pipette was repositioned, and the stimulus intensity was adjusted until the current required to elicit an all-or-none response was minimized. Parallel fibers were stimulated by placing a patch pipette filled with bath solution in the molecular layer and adjusting the stimulus intensity until the desired input was reached. Parallel fiber input was distinguished from climbing fiber input by the amplitude, pair-pulse facilitation and slower decay kinetics of the parallel fiber–evoked AMPAR EPSCs. For the experiments in **Figure 5c–e**, we have pooled the results from 50 μM and 100 μM TBOA, as there was no significant difference. In the

presence of 50 μM TBOA, mGluR EPSCs were 224 ± 99 pA in lobule III ($n = 4$) and 233 ± 102 pA in lobule X ($n = 6$). In 100 μM TBOA, mGluR EPSCs were 293 ± 58 pA in lobule III ($n = 5$) and 244 ± 28 pA in lobule X ($n = 3$; $P = 0.55$ and $P = 0.94$ for each lobule). For the experiments in **Figure 6a–d**, spontaneous IPSCs (sIPSCs) were recorded by omitting picrotoxin or SR95531 from the recording medium and including NBQX (10 μM) to block AMPAR-mediated EPSCs. sIPSCs were detected using a synaptic template and were divided, for each trial, into 2-s bins. The charge of the sIPSCs falling into corresponding bins was summed. The charge transfer in each bin was then normalized to the average charge calculated over the control baseline period of 10 s (5 bins). Calculation of the maximal inhibition due to either mGluR activation or depolarization (DSI; 1 s from –60 to 0 mV) was quantified by calculating synaptic charge in 5-s bins (between 6–11 s post-stimulus). For LTD experiments (conducted at 32–34 °C), the parallel fiber EPSCs were elicited at 0.5 Hz. Induction of LTD was accomplished by a pairing depolarization of the Purkinje cell to 0 mV for 100 ms and stimulation of the parallel fibers with trains (ten pulses at 100 Hz) every 2 s for 2 min. Synaptic currents were filtered at 2–5 kHz and digitized at 20–50 kHz using acquisition software written in Igor Pro software (J.S. Diamond; WaveMetrics). Reported values are the mean ± s.e.m. Data analysis was done using Igor Pro and AxoGraph (Axon Instruments). Recordings were performed at room temperature (23–25 °C), in the presence of 100 μM picrotoxin, unless otherwise noted. For each experimental protocol, we alternated recordings from Purkinje cells in lobule III with those in lobule X during each day. Thus, the comparisons of properties across lobules were internally controlled for the age of the animal and slice health.

ACKNOWLEDGMENTS

We thank the members of the Jahr lab, L.O. Wadiche and A.V. Tzingounis for comments and suggestions during this project. Supported by NS40056 (C.E.J.).

COMPETING INTERESTS STATEMENT

The authors declare that they have no competing financial interests.

Published online at http://www.nature.com/natureneuroscience/
Reprints and permissions information is available online at http://npg.nature.com/reprintsandpermissions/

1. Bergles, D.E., Diamond, J.S. & Jahr, C.E. Clearance of glutamate inside the synapse and beyond. *Curr. Opin. Neurobiol.* **9**, 293–298 (1999).
2. Danbolt, N.C. Glutamate uptake. *Prog. Neurobiol.* **65**, 1–105 (2001).
3. Auger, C. & Attwell, D. Fast removal of synaptic glutamate by postsynaptic transporters. *Neuron* **28**, 547–558 (2000).
4. Tanaka, K. *et al.* Epilepsy and exacerbation of brain injury in mice lacking the glutamate transporter GLT-1. *Science* **276**, 1699–1702 (1997).
5. Brasnjo, G. & Otis, T.S. Neuronal glutamate transporters control activation of postsynaptic metabotropic glutamate receptors and influence cerebellar long-term depression. *Neuron* **31**, 607–616 (2001).
6. Diamond, J.S. Neuronal glutamate transporters limit activation of NMDA receptors by neurotransmitter spillover on CA1 pyramidal cells. *J. Neurosci.* **21**, 8328–8338 (2001).
7. Huang, Y.H., Dykes-Hoberg, M., Tanaka, K., Rothstein, J.D. & Bergles, D.E. Climbing fiber activation of EAAT4 transporters and kainate receptors in cerebellar Purkinje cells. *J. Neurosci.* **24**, 103–111 (2004).
8. Jackson, M. *et al.* Modulation of the neuronal glutamate transporter EAAT4 by two interacting proteins. *Nature* **410**, 89–93 (2001).
9. Casado, M. *et al.* Phosphorylation and modulation of brain glutamate transporters by protein kinase C. *J. Biol. Chem.* **268**, 27313–27317 (1993).
10. Konnerth, A., Llano, I. & Armstrong, C.M. Synaptic currents in cerebellar Purkinje cells. *Proc. Natl. Acad. Sci. USA* **87**, 2662–2665 (1990).
11. Perkel, D.J., Hestrin, S., Sah, P. & Nicoll, R.A. Excitatory synaptic currents in Purkinje cells. *Proc. Biol. Sci.* **241**, 116–121 (1990).
12. Wadiche, J.I. & Jahr, C.E. Multivesicular release at climbing fiber-Purkinje cell synapses. *Neuron* **32**, 301–313 (2001).
13. Otis, T.S., Kavanaugh, M.P. & Jahr, C.E. Postsynaptic glutamate transport at the climbing fiber-Purkinje cell synapse. *Science* **277**, 1515–1518 (1997).
14. Fairman, W.A., Vandenberg, R.J., Arriza, J.L., Kavanaugh, M.P. & Amara, S.G. An excitatory amino-acid transporter with properties of a ligand-gated chloride channel. *Nature* **375**, 599–603 (1995).
15. Wadiche, J.I., Amara, S.G. & Kavanaugh, M.P. Ion fluxes associated with excitatory amino acid transport. *Neuron* **15**, 721–728 (1995).
16. Bergles, D.E., Tzingounis, A.V. & Jahr, C.E. Comparison of coupled and uncoupled currents during glutamate uptake by GLT-1 transporters. *J. Neurosci.* **22**, 10153–10162 (2002).
17. Dzubay, J.A. & Jahr, C.E. The concentration of synaptically released glutamate outside of the climbing fiber-Purkinje cell synaptic cleft. *J. Neurosci.* **19**, 5265–5274 (1999).
18. Nagao, S., Kwak, S. & Kanazawa, I. EAAT4, a glutamate transporter with properties of a chloride channel, is predominantly localized in Purkinje cell dendrites, and forms parasagittal compartments in rat cerebellum. *Neuroscience* **78**, 929–933 (1997).
19. Dehnes, Y. *et al.* The glutamate transporter EAAT4 in rat cerebellar Purkinje cells: a glutamate-gated chloride channel concentrated near the synapse in parts of the dendritic membrane facing astroglia. *J. Neurosci.* **18**, 3606–3619 (1998).
20. Welsh, J.P. *et al.* Why do Purkinje cells die so easily after global brain ischemia? Aldolase C, EAAT4, and the cerebellar contribution to posthypoxic myoclonus. *Adv. Neurol.* **89**, 331–359 (2002).
21. Lehre, K.P., Levy, L.M., Ottersen, O.P., Storm-Mathisen, J. & Danbolt, N.C. Differential expression of two glial glutamate transporters in the rat brain: quantitative and immunocytochemical observations. *J. Neurosci.* **15**, 1835–1853 (1995).
22. Ozol, K., Hayden, J.M., Oberdick, J. & Hawkes, R. Transverse zones in the vermis of the mouse cerebellum. *J. Comp. Neurol.* **412**, 95–111 (1999).
23. Foster, K.A., Kreitzer, A.C. & Regehr, W.G. Interaction of postsynaptic receptor saturation with presynaptic mechanisms produces a reliable synapse. *Neuron* **36**, 1115–1126 (2002).
24. Delaney, A.J. & Jahr, C.E. Kainate receptors differentially regulate release at two parallel fiber synapses. *Neuron* **36**, 475–482 (2002).
25. Baude, A. *et al.* The metabotropic glutamate receptor (mGluR1 alpha) is concentrated at perisynaptic membrane of neuronal subpopulations as detected by immunogold reaction. *Neuron* **11**, 771–787 (1993).
26. Batchelor, A.M. & Garthwaite, J. Frequency detection and temporally dispersed synaptic signal association through a metabotropic glutamate receptor pathway. *Nature* **385**, 74–77 (1997).
27. Kim, S.J. *et al.* Activation of the TRPC1 cation channel by metabotropic glutamate receptor mGluR1. *Nature* **426**, 285–291 (2003).
28. Takayasu, Y., Iino, M. & Ozawa, S. Roles of glutamate transporters in shaping excitatory synaptic currents in cerebellar Purkinje cells. *Eur. J. Neurosci.* **19**, 1285–1295 (2004).
29. Galante, M. & Diana, M.A. Group I metabotropic glutamate receptors inhibit GABA release at interneuron-Purkinje cell synapses through endocannabinoid production. *J. Neurosci.* **24**, 4865–4874 (2004).
30. Kreitzer, A.C. & Regehr, W.G. Cerebellar depolarization-induced suppression of inhibition is mediated by endogenous cannabinoids. *J. Neurosci.* **21**, RC174 (2001).
31. Crepel, F. & Jaillard, D. Pairing of pre- and postsynaptic activities in cerebellar Purkinje cells induces long-term changes in synaptic efficacy *in vitro*. *J. Physiol. (Lond.)* **432**, 123–141 (1991).
32. Linden, D.J., Dickinson, M.H., Smeyne, M. & Connor, J.A. A long-term depression of AMPA currents in cultured cerebellar Purkinje neurons. *Neuron* **7**, 81–89 (1991).
33. Ito, M. The molecular organization of cerebellar long-term depression. *Nat. Rev. Neurosci.* **3**, 896–902 (2002).
34. Wang, Y.T. & Linden, D.J. Expression of cerebellar long-term depression requires postsynaptic clathrin-mediated endocytosis. *Neuron* **25**, 635–647 (2000).
35. Aiba, A. *et al.* Deficient cerebellar long-term depression and impaired motor learning in mGluR1 mutant mice. *Cell* **79**, 377–388 (1994).
36. Hansel, C., Linden, D.J. & D'Angelo, E. Beyond parallel fiber LTD: the diversity of synaptic and non-synaptic plasticity in the cerebellum. *Nat. Neurosci.* **4**, 467–475 (2001).
37. Kano, M. *et al.* Persistent multiple climbing fiber innervation of cerebellar Purkinje cells in mice lacking mGluR1. *Neuron* **18**, 71–79 (1997).
38. Ichise, T. *et al.* mGluR1 in cerebellar Purkinje cells essential for long-term depression, synapse elimination, and motor coordination. *Science* **288**, 1832–1835 (2000).
39. Finch, E.A. & Augustine, G.J. Local calcium signaling by inositol-1,4,5-trisphosphate in Purkinje cell dendrites. *Nature* **396**, 753–756 (1998).
40. Wang, S.S., Denk, W. & Hausser, M. Coincidence detection in single dendritic spines mediated by calcium release. *Nat. Neurosci.* **3**, 1266–1273 (2000).
41. Nishiyama, H. & Linden, D.J. Differential maturation of climbing fiber innervation in cerebellar vermis. *J. Neurosci.* **24**, 3926–3932 (2004).
42. Brochu, G., Maler, L. & Hawkes, R. Zebrin II: a polypeptide antigen expressed selectively by Purkinje cells reveals compartments in rat and fish cerebellum. *J. Comp. Neurol.* **291**, 538–552 (1990).
43. Fritschy, J.M. *et al.* GABAB-receptor splice variants GB1a and GB1b in rat brain: developmental regulation, cellular distribution and extrasynaptic localization. *Eur. J. Neurosci.* **11**, 761–768 (1999).
44. Jinno, S., Jeromin, A., Roder, J. & Kosaka, T. Compartmentation of the mouse cerebellar cortex by neuronal calcium sensor-1. *J. Comp. Neurol.* **458**, 412–424 (2003).
45. Harrison, J. & Jahr, C.E. Receptor occupancy limits synaptic depression at climbing fiber synapses. *J. Neurosci.* **23**, 377–383 (2003).
46. Levenson, J. *et al.* Long-term potentiation and contextual fear conditioning increase neuronal glutamate uptake. *Nat. Neurosci.* **5**, 155–161 (2002).